

## Deployable Optical Receiver Array Cubesat

Adriana Talamante, Judd D. Bowman, Daniel C. Jacobs, Zachary Hoffman, Michael Horne, Christopher McCormick

School of Earth and Space Exploration, Arizona State University  
781 E Terrace Mall, Tempe 85282; 480-965-8880  
atalama1@asu.edu, daniel.c.jacobs@asu.edu

Jose E. Velazco, Julia Arnold, Sean E. Cornish, Uriel S. Escobar, Andy R. Klaib

Jet Propulsion Laboratory  
4800 Oak Grove Dr., Pasadena, CA 91109; 818-354-4605  
jose.e.velazco@jpl.nasa.gov

### ABSTRACT

Small satellites and cubesats often have low data transmission rates due to the use of low-gain radio links in UHF and S bands. These links typically provide up to only 1 Mbps for communication between the ground and LEO, limiting the applications and mission operations of small satellites. Optical communication technology can enable much higher data rates and is rapidly gaining hold for larger satellites, including for crosslinks within SpaceX's Starlink constellation and upcoming NASA deep space missions. However, it has been difficult to implement on small satellites and cubesats due to the need for precision pointing on the order of arcseconds to align the narrow optical laser beam between terminals--a laser transmitter in LEO may yield a footprint less than 100 meters wide at its receiving ground station. We report the development of a 3U cubesat to demonstrate new optical communication technology that eliminates precision pointing accuracy requirements on the host spacecraft. The deployable optical receiver aperture (DORA) aims to demonstrate 1 Gbps data rates over distances of thousands of kilometers. DORA requires an easily accommodated host pointing accuracy of only 10 degrees with minimal stability, allowing the primary mission to continue without reorienting to communicate and/or enabling small satellite missions using low-cost off-the-shelf ADCS systems. To achieve this performance, DORA replaces the traditional receiving telescope on the spacecraft with a collection of wide-angle photodiodes that can identify the angle of arrival for incoming communication lasers and steer the onboard transmitting laser in the corresponding direction. This work is motivated by NASA's plans for a lunar communications and navigation network and supported by NASA's Space Technology Program (STP). It is ideally suited for crosslink communications among small spacecraft, especially for those forming a swarm and/or a constellation, and for surface to orbit communications. We will implement the deployable optical receiver aperture and miniature transmission telescope as a 1U payload in the 3U cubesat and conduct the demonstration flight in LEO. Future implementations of the DORA technology are expected to further enable omnidirectional receiving of multiple optical communications simultaneously and accommodate multiple transmitting modules on a single cubesat.

### INTRODUCTION

Spacecraft clusters and optical communications may enable paradigm-shifting compact instrumentation and high-speed communications capabilities for missions ranging from low-Earth and cis-lunar orbit to the outer planets in deep space. NASA exploration plans require spacecraft in cis-lunar space and users on the lunar surface to have reliable and simple access to high bandwidth communication. The network providing this service may be a mix of assets with a layered hierarchical structure like the tiered connections in terrestrial networks. Given current and projected use patterns, smallsats up to 12U in size are envisioned to be a key user and node participant in this relay network. However,

at this size scale, collecting area and pointing flexibility are both extremely limited. Deployable apertures, like the X-band reflect-array used on the MarCO cubesat are able to provide sufficient gain to enable 8 kbps links at 1 AU, while the LunaH-Map cubesat will communicate over X-band from the Moon back to Earth at 128 kbps. Both of these missions offset their minimal collecting area with the use of a large (34m/70m) Deep Space Network (DSN) dish on Earth. Direct communication between cis-lunar elements can benefit from much shorter distances to achieve speeds in the ~5 Mbps range in the same radio band. These can be relayed further distances by traversing the node network, potentially waiting for connection opportunities along the way, until

arriving at a more powerful transmitter. Data could traverse this architecture according to a Delay Tolerant Network (DTN) protocol (Burleigh, et al 2003).

Traditional laser terminals employed to date use lenses to gather incoming light onto a single sensor. This optical setup uses a significant internal spacecraft volume for the optical path and is limited in collecting area to the size of the lens aperture. This imposes two constraints. First, and most seriously, in a lens terminal the operable field of view is limited to a small range set by the focal length of the telescope, typically less than a few degrees. Second, a lens-based system is typically limited in its pointing capability, which then imposes strict pointing requirements on the host spacecraft. A LEO station with a typical beam dispersion requires milli-radian angular control from the cubesat pointing system, which must be locked to the optical terminal, making other pointing operations impossible. The tight integration and control of pointing makes a traditional laser terminal a significant driver of a cubesat mission's architecture (Cahoy et al. 2019).

An alternative optical architecture is the wide-field laser terminal. The basic concept uses arrays of silicon photodiodes to receive laser signals incoming from any direction. The diode array can be used to estimate the direction of arrival of the incoming signal either by making spatial measurements of the incoming beam profile or by exploiting the directional dependence of the diode response. The arrival angle is then used to steer the return link beam with an actuated mirror.

The basic concept of a wide-field laser terminal can be utilized in several ways onboard a small satellite. A large number of small sensors can be tiled onto a sphere or multi-faceted surface to provide a large number of simultaneous connections from different directions (Velazco et al., 2018, 2019). Alternatively, to service longer links where more sensitivity and tighter pointing determination is needed, the collecting area can be tiled onto a planar surface, such as a deployable panel (or panels), to provide a large collecting area. This is the design we will demonstrate with the Deployable Optical Receiver Aperture (DORA) cubesat.

Small spacecraft, such as cubesats, often use small communication apertures that conform to the spacecraft body. For instance, in a cubesat, conformal apertures are typically limited to a 10 cm diameter (77 cm<sup>2</sup> collecting area). The DORA cubesat will demonstrate a deployable receive aperture with the potential for a 7x improvement in collecting area that fits within 1U, enabling higher data rates and/or longer communication distances than traditional systems.

In the following sections, we begin by reviewing the project and its goals. We next describe the DORA payload, including its heritage and current design. We end with an overview of the spacecraft bus.

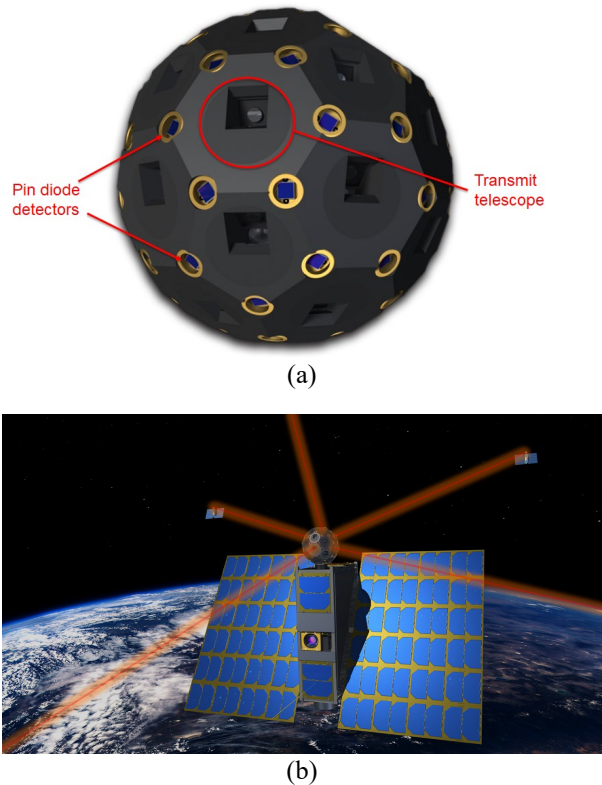


**Figure 1: Rendered images of (a) ISOC and (b) constellation of spacecraft interconnected by ISOC.**

## PROJECT OVERVIEW

The Jet Propulsion Laboratory has previously developed the omnidirectional Inter-Satellite Optical Communicator (ISOC), a novel omnidirectional optical terminal to provide fast communications for constellations of spacecraft (Velazco et al., 2018). The ISOC features a truncated icosahedral geometry that contains arrays of miniature laser telescopes and optical detectors (see Figure 1). The miniature optical telescopes are located at the center of each facet and allow for full sky coverage. The optical detectors, symmetrically deployed on each vertex of the ISOC body, have two purposes: they allow receiving fast incoming communications signals from any direction and they are used to accurately determine the angle-of-arrival (AoA) of the incoming signal. The constant AoA tracking performed by the ISOC mechanism makes it ideally suited for ground station pointing operations as well. The ISOC main features are: 1) high data rate communications, 2) full sky coverage and 3) its ability to maintain multiple links simultaneously. The current

ISOC prototype operates at a wavelength of 650 nm (1550 nm is in development) and uses low-power single mode laser diodes with fast silicon photodetectors. It has been tested in the laboratory, giving the system a technology readiness level (TRL) of 3.

### Objectives and Requirements

The DORA cubesat objective is a flight demonstration of a laser terminal that supports 1000 km crosslinks without precision spacecraft pointing. We expect to raise the widefield optical communication technology to TRL 7. To avoid the difficulty posed by using multiple spacecraft for the initial demonstration, we have elected to make the test between a ground terminal and a single 3U cubesat in LEO. The overall goal of the mission is to demonstrate link performance, which we have broken into key performance parameters listed in Table 1. Required levels are set by the desired performance across several potential applications. We also identify target levels beyond requirements that are our design goals.

Table 1 — DORA performance requirements

Parameter	Required	Target
KPP #1 - Angle of arrival accuracy	20"	5"
KPP #2 - Tx pointing accuracy	20"	5"
KPP #3 - Allowed bus drift rate	0.1° / s	1° / s
KPP #4 - Allowed off-axis angle	5°	36°
KPP #5 - Sustained data rate	0.5 Gbps	1 Gbps
KPP #6 - Bit error rate (BER)	10 <sup>-8</sup>	10 <sup>-9</sup>
Transmit power	1 W	2 W
Transmit optics collimation	100"	20"
Stray light rejection (sun angle)	90°	30°

The DORA terminal, described in more detail below, works by determining the angle of arrival of an incoming laser and steering its transmitter laser to close the bidirectional link. Thus, a successful uplink is required before downlink can occur. The mission concept of operations and test phases (Figure 2) set receiver demonstration highest priority with full bidirectional link to come after. The overall mission operational approach is to perform link experiments when the cubesat is above the experimental ground terminal. Experiments will be mainly at night, when solar background is at a minimum.

Initially, the optical receiver will be tested using feedback via radio to find and calibrate the orbiting terminal. This will also refine the pointing calibration of

the ground transmitter. Calibration products will depend on the bench top optimization before launch but are likely to be expressed as an overall pointing offset. Sustained link speed will be demonstrated by upload of a file with accuracy tested by on-board hash calculation.

Transmitter testing will require much the same process as the receiver with a search process to find the ground receiver and calibrate pointing at both ends. Verification plans include high speed download, and because the link is continuously bidirectional, live round-trip data.

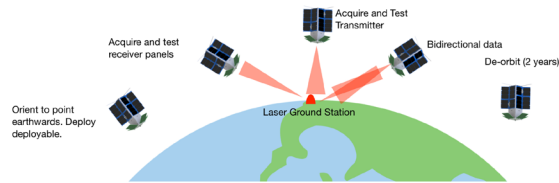


Figure 2: Mission test phases

The angular accuracy of the combined receiver transmitter system sets operational range as well as the required pointing accuracy of the cubesat host. The transmitter angular tracking requirements (KPP1 and 2) are set to give a five meter pointing error at 1000 km, well inside the projected laser spot size of about 500 meters at that distance. Similarly, tolerance of spacecraft bus angular drift rate of 1 deg/s or slower is a tumble rate reasonably achievable with off-the-shelf attitude control systems.

Many factors including receiver sensitivity, transmitter power, angular error, and processor latency contribute to the overall link performance. The primary performance metric for a crosslink in a cubesat acting as a communication node is the data rate that can be achieved within a cost-effective mission architecture. Here we focus on the sustained link speed attainable between two identical small satellite terminals at 1000 km with 10 degree host bus pointing accuracy and stability. Without the proposed technology a 1000 km link would be closed by an X-band patch antenna crosslink at 0.1 to 1 Mbps, depending on power levels, while existing optical systems would not close the link due to the low pointing stability of the cubesat. The DORA system is expected to sustain the link at better than 1 Gbps, approximately three orders of magnitude larger than X-band. This data rate enhancement offers a significant improvement over the hundreds of kbps which is the projected state of the art for cubesat missions on the first cis-lunar missions.

### DORA PAYLOAD MODULE

The DORA payload is a 1U module that contains both the optical receiver and laser transmitter functionality. The module has four deployable square-shaped tiles and

one face-mounted tile for receiving incoming laser signals. Each tile contains dozens of fast optical detectors. The outputs of all detectors in each tile pass through suitable impedance matching transformers and are then power-combined to make up one large effective collecting area for each tile. We plan to explore both silicon pin diodes and silicon photomultiplier (SiPM) detectors for this application. State of the art commercial pin diodes and SiPMs are fast (1 GHz bandwidth) and are available in sizes up to 3 x 3 mm. The array of five square-shaped tiles, each with an area of 100 cm<sup>2</sup>, yields a total possible DORA aperture of 500 cm<sup>2</sup>. However, for the purposes of an initial demonstration we do not need to fully populate the receiver tiles with SiPMs. We will use only a total SiPM area of 6.4 cm<sup>2</sup>, equivalent to 1.3% of the total possible aperture. Renderings of the DORA payload module are shown in Figure 3.

The DORA payload will determine the incoming laser AoA using the direction dependent response of the SiPMs. The SiPMs sensitivity decreases for arrival angles away from the boresight direction with cosine dependence. The deployable panels will be tilted relative to each other (and the top face) to provide multiple SiPM orientations. This will enable the two-dimensional AoA to be calculated from the relative incoming laser strength seen by each panel.

The laser transmitter is a miniature telescope that consists of a laser diode, a fixed mirror, an actuated mirror, and a 3x bi-confocal lens. The actuated mirror provides an optical steering range of  $\pm 12^\circ$ . The 3x lens expands the steering to  $\pm 36^\circ$ . Although the proposed demonstration cubesat will contain only one transmitter, a communication node spacecraft could contain multiple strategically located telescopes to provide full sky coverage. Two identical spacecraft, each containing a DORA system with transmit module radiating 1 Watt (at 850 nm) with a transmitting aperture of 0.8 cm<sup>2</sup>, should be able to communicate at 1 Gbps data rate (using NRZ OOK modulation) at 5,000 kilometers with a bit error rate (BER) of  $10^{-8}$ .

### ***Optical and Electrical Design***

The DORA receiving tiles are each an 83 x 100 mm printed circuit board (PCB) that hosts the SiPMs, RF combiners, amplifiers, biasing circuit, and connector. An optical filter will be mounted on top of each panel to mitigate background light as described below. All other components are either surface mounted onto the tile PCBs or contained on additional PCBs in the 1U module.

SiPMs are optical sensors that are composed of multiple single photon avalanche diodes (SPAD) connected in parallel. A SPAD is a PN junction photodiode that is biased to operate in the Geiger mode. The Geiger mode

allows for impact ionization to occur, creating gains up to  $10^6$ . SPADs are often referred to as the microcells in the SiPM. Each SiPM outputs a current signal that is proportional to the number of microcells fired. A fired microcell outputs a pulse of 1 photoelectron (p.e.). When more than one microcell fires at the same time, the output of the SiPM is the superposition of all the fired cells. There are two outputs for each SiPM, a standard output and fast output. The standard output is the typical photodetector current from the anode and will be used to observe the DC level of the signal for use in the AoA calculation. The fast output will be used for communication.

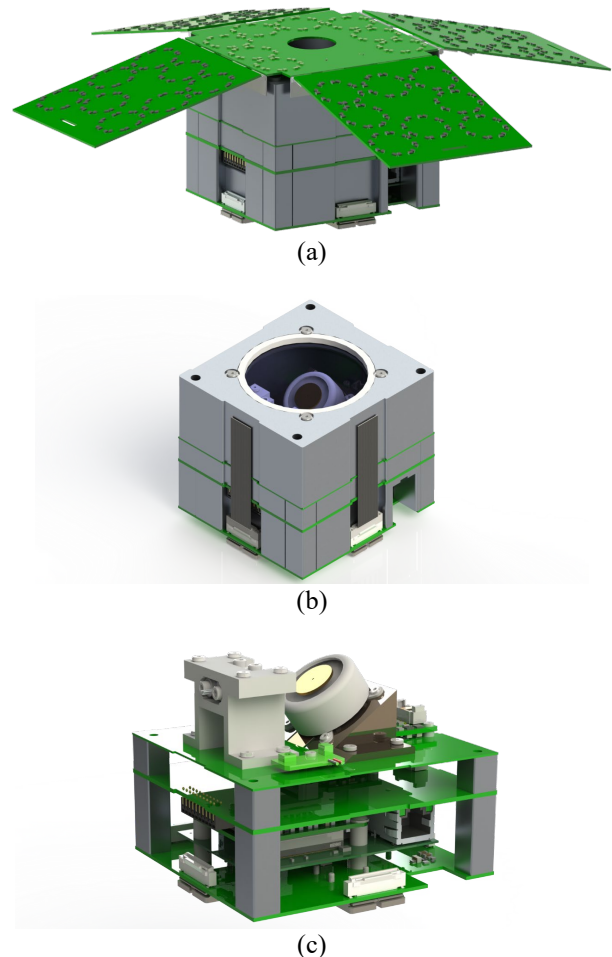


**Figure 3: DORA payload 1U module. (a) Shown in full with optical receiver panels deployed. (b) Shown with receiver panels hidden. The actuated mirror for steering the transmitter laser is visible through the top face. (c) Shown with panels and thermal shields hidden, revealing the analog and digital processing boards.**

Biasing is important for SiPM, as its dark current, gain, and photon detection efficiency are all dependent on it.

To achieve the proper biasing voltages a DC-DC inverter (LT3483) is used to generate a voltage range of -30 V to -20 V from a 3.3 V or 5 V line. Temperature affects the required biasing due to the change in breakdown voltage. A DC-DC inverter has a variable output voltage that is being controlled by a feedback resistor. A thermistor is used as the feedback resistor so that the change in resistance due to the change in temperature changes the bias voltage at the same rate that the breakdown voltage changes.

The front-end electronics of a SiPM are similar to those for an avalanche photodiode, the only exception is that the SiPM has two outputs. The outputs must be converted from a current signal to a voltage signal in order to be sampled by an analog-to-digital converter (ADC) or comparator. A transimpedance amplifier (TIA) is used to convert the current signal to voltage signal, as well as providing additional gain. Before connecting the SiPM outputs to the TIA each fast output will connect to an RF combiner. Combining the individual signals will improve SNR by increasing the peak of the output pulse. The RF combiner also provides isolation, which lowers the sum capacitive load when connecting the outputs together. The RF combiner output is then connected to the TIA. The output of the TIA connects to a comparator which converts the analog output signal of the TIA into a digital signal. Each panel will have a flat flexible cable (FFC) connector that is used to connect it to a digital processing board. The FFC connector and cable allow for thin cabling that reduces the thickness of the panels.

The DORA payload utilizes a Kintex-7 FPGA on a Trenz Electronic TE0741 system-on-module (SOM) for managing the optical communications link. The SOM attaches to a custom-designed carrier card using three board-to-board connectors. The carrier card provides several interfaces, including an RS-422 driver, a microSD card slot, and an Ethernet PHY and transformer. The RS-422 bus is used to control the payload from the CubeSat's flight computer, and the Ethernet interface is used to transfer files between the flight computer and the payload. The microSD card is used to hold files for later transmission and to save files that have been received. The carrier card also contains a 512 Mb Cypress HyperRAM module, which serves as a data buffer during an optical link.

The carrier card connects to a mixed signal PCB (MS-PCB) using a 60-pin Samtec Razor Beam High-Speed connector. The high-speed GTX transceivers of the Kintex-7, along with several GPIO and an SPI interface, are routed through this connector. The GTX transceivers are used to modulate the transmit laser, and to recover data from the SiPM panels. The SPI interface is used to

retrieve samples from the MS-PCB's Analog Devices AD7606C-18 ADC, and to command the Optotune dual-axis voice-coil mirror to steer the transmitter laser beam.

The MS-PCB interconnects the FPGA carrier card, receiver tiles, laser transmitter, ADC, and Optotune mirror carrier board, along with hosting burn wires for receiver tile deployments and all power lines for the payload. Five FCC connectors/cables are used in order to connect each receiver tile to the MS-PCB and additionally one of the five FCC connectors supplies power and the transmitter signal to the laser transmitter board. A 16 pin Harwin connector is used for power and control interface with the Optotune mirror carrier board. The burn wires are located on the underside of the board.

The FPGA implements a MicroBlaze soft-core processor running FreeRTOS. The communications logic, Ethernet MAC, HyperRAM controller, UART core, and SPI logic are all connected to the processor using an AXI-4 bus. The Xilinx EthernetLite IP is used as the Ethernet MAC and the Xilinx UartLite IP is used to provide the data layer for the RS-422 interface. The processor is responsible for controlling the payload's file system, implementing the TCP/IP Ethernet stack, parsing RS-422 commands, and managing the communications link.

### *Mechanical Design*

The DORA payload consists of a series of sub-boards depicted in Figure 4. The optical transmitter allows for a modulated laser diode to emit a pulsed beam from the block enclosure, horizontally into the center of the steering mirror. The steering mirror sits at a platform elevated 35° above horizontal. This enables the  $\pm 25^\circ$  mechanical range of the mirror to steer the beam without clipping the cubesat structure.

To assemble the payload in an effective manner, spacers and standoffs were created, similar to the 0.6" spacers outlined in the CubeSat Design Specification Revision 13 (CDS; 2015). However, with the volume of the payload in mind, the spacers were shortened, allowing for a more efficient volume board stack.

In addition to the spacers, corner mounting brackets are needed to add rigidity to the structure and give the stack a more functional way to mount to the cubesat chassis. The rectangular corner brackets, seen in Figure 4 (bottom panel), give the payload a more vibration resistant design, and give additional material for mounting to the chassis and conducting heat.

To keep all electrical components within an operational thermal range, shells of Aluminum 7050-T73510 were designed to shield components from direct sun exposure

and keep them within an enclosed system (Starke 1996). The shields, seen in Figure 3 (middle panel), allow for a closed payload system, preventing overheating or accidental tampering, only added an additional 0.67 kg to the payload mass. The overall payload mass is 1.1 kg.

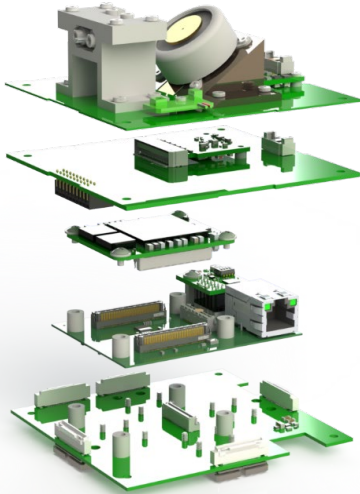


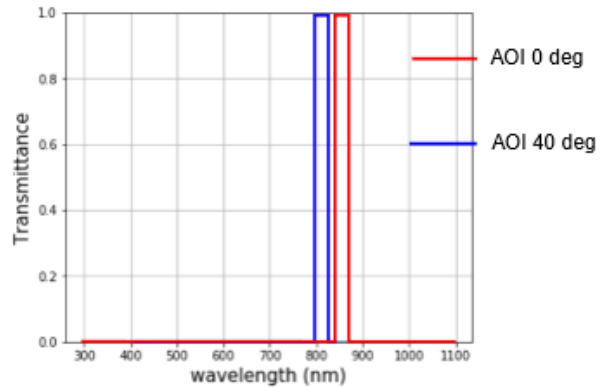
**Figure 4: Exploded view of the DORA payload module. From bottom to top, the boards are: 1) MS-PCB, 2) SOM carrier card, 3) FPGA, 4) laser modulator, and 5) laser transmitter with *Optotune* steering mirror.**

The glass cover over the transmitter is shown in Figure 3 (middle panel) in blue to highlight its presence. In application; however; the cover will be a clear glass of a known index of refraction to ensure all potential pointing errors are accounted for and no additional loss is accrued due to filtering.

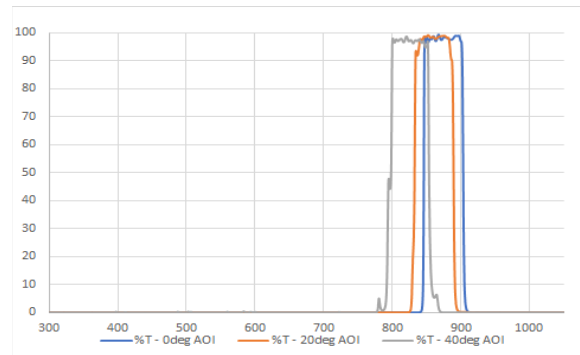
The most prominent features on the DORA module are the deployable receiver tiles. These panels spring out from the cubesat body in a flower-petal fashion as seen in Figure 3 (top panel). The panels provide an opportunity for a large optical aperture for an incoming signal from the ground or other spacecraft. Although we are not fully populating the panels with diodes, we retain them in the design to test their impact on the AoA determination. Each panel is held rigidly in reference to one another by the hinges that connect them to the body of the cubesat. The hinges are spring loaded, and will launch from the initial stowed position to a preset 70° angle, similar to the deployable Ka reflector on JPL’s ISARA mission (Hodges 2015). The hinges also meet the thickness requirements for normal extension from the cubesat body as defined in the CDS.

When DORA is launched, the receiver panels will be down, covering the sides of the payload until the cubesat

is in its proper orbit. When orbit is achieved, the burn wire mechanisms on each side of the payload will send a high current through a nichrome wire, burning a taut nylon cord that is keeping the panels from deploying. The burn wire mechanisms can be seen below the connectors on the underside of the MS-PCB in Figure 4, and will connect to each panel via the slot at the end of each PCB.



(a)



(b)

**Figure 5: (a) Illustration of the shift in passband for a 850 nm bandpass filter with a bandwidth of 20 nm for two different incidence angles. (b) An actual bandpass filter transmission with a passband of ~50 nm for the same two incidence angles is able to retain high response at the target wavelength in both cases.**

## BACKGROUND LIGHT MITIGATION

Background light will contribute to the power received by DORA and its ground station. The large field of view (about  $\pi$  steradians) of the DORA receiver makes it more susceptible to background light than narrow field systems for two reasons: 1) bright sources are more likely to be in the field of view and 2) diffuse background emission will integrate to larger power than for narrow field of view systems. Additionally, photodiode

detectors have broadband response (~500 nm) unless filters or coatings are applied. Hence, thermal and other broadband background light sources can integrate to large power in these detectors.

Calculations show that for either Silicon detector systems, atmospheric line emission (e.g. OH lines) and light pollution may be a significant or even dominant contribution to the received power of a DORA system on the ground or in LEO. Diffuse astronomical sources, such as Zodiacal light and faint stars, are generally not dominant sources of background light.

We use optical bandpass filters to increase the SNR by reducing the background noise observed by the detector. The bandpass filter reduces the transmission of unwanted optical bands (reject band) and allows high transmission of the desired optical wavelength (passband). Typical transmittance of the passband is above 90% while the reject band provides 30 dB attenuation. Filters experience a “blueshift” when an incidence angle is larger than the intended operating angle. Figure 5 shows an example of how the blueshift changes the performance of the filter.

In order for the filter to maintain a >90% transmission for an incidence angle range of 0 to 40 degrees, the bandwidth of the passband must be increased. The lower panel of Figure 5 illustrates how a larger passband can achieve large angle ranges.

### Summary of link budget derivation

In Figure 6 we show the basic transmit and receive terminals separated by a distance  $R$ . The transmit telescope includes a laser diode and a collimating aperture (transmit aperture). The receiver includes a receive lens (receive aperture) and a photodetector. For an optical terminal the received power can be calculated as,

$$P_r = P_t \left( \frac{\pi D_t}{\lambda} \right)^2 \left( \frac{\pi D_r}{\lambda} \right)^2 \left( \frac{\lambda}{4\pi R} \right)^2 \eta, \quad (1)$$

where we have neglected losses. Here  $P_t$  is the transmitted power,  $D_t$  and  $D_r$  are, respectively, the transmit and receive effective aperture diameters,  $\lambda$  is the operating wavelength,  $R$  is the distance between terminals and  $\eta$  is the system efficiency. Equation 1 can be rewritten as

$$P_r = E G L \eta, \quad (2)$$

where  $E = P_t (\pi D_t / \lambda)^2$  is the effective isotropic radiated power. The receive gain and space loss are given by respectively by:

$$G = \left( \frac{\pi D_r}{\lambda} \right)^2, \quad (3)$$

$$L = \left( \frac{\lambda}{4\pi R} \right)^2. \quad (4)$$

Assuming direct detection optical links, the capacity of a Poisson pulse position modulation (PPM) channel is a function of the PPM order, received noise and signal rates. When only signal photoelectrons are present, we have

$$C_{OPT} = \frac{\log_2(M)}{M T_s} [1 - e^{-M P_r T_s / E_\lambda}], \quad (4)$$

where  $M$  is the PPM order,  $T_s$  is the slot width, and  $E_\lambda = hc/\lambda$  is the energy per photon ( $h$  is Planck’s constant and  $c$  is the speed of light). The maximum supportable bandwidth,  $1/T_s$ , is typically limited by the maximum processing speed of the transmitter and receiver, the laser pulse width, and clock accuracy. Figure 7 shows that the expected data rate for the DORA payload module transmitting to a ground station will sustain 1 Gbps for distances less than 1800 km.

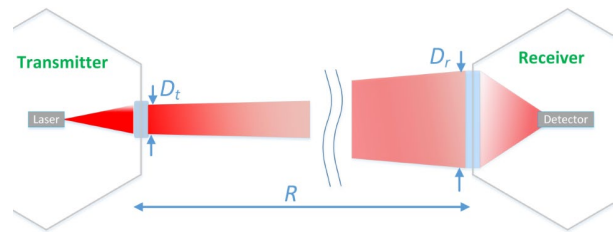


**Figure 6. Transmitter and receiver terminals showing relevant parameters for DORA optical communications.**

### SPACECRAFT BUS

The cubesat will be 3U and use standard subsystems for the electrical and power system, attitude control and determination system, GPS receiver and antenna, onboard computing, and UHF radio and antenna (see Figure 8). The electronics subsystems are a mix of commercial off the shelf (COTS) and custom design with several items still under trade study. The chassis is a custom machined design. Power will be supplied by two 100 x 200 mm chassis-mounted solar panels and two 100 x 200 mm deployable solar panels, yielding a total orbital average power output of 7.4 W. Average power consumption for all bus subsystems and the DORA payload, including efficiency loss, is estimated at 3.3 W, providing 120% margin. We estimate the payload will consume 8.5 W when transmitting. The operational duty cycle for on-orbit testing will be 5% (4 night passes per 24 hours), yielding an orbital average power consumption for the payload of 0.43 W.

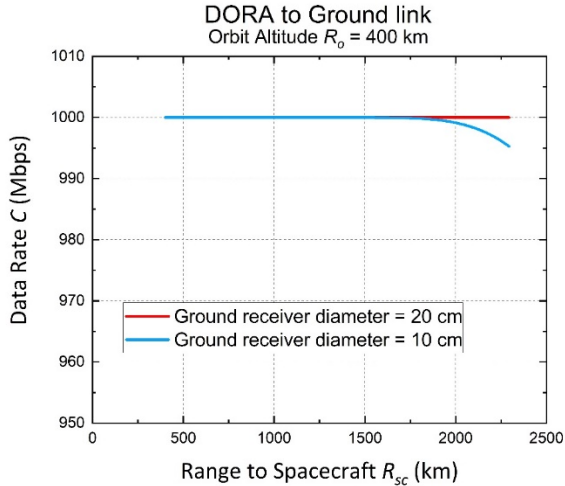


**Figure 7: Plot of capacity (Equation 4) as a function of range for the DORA payload to the ground station, for two values of the ground station receive aperture,  $D_r = [10, 20]$  cm. Parameters used are:  $\lambda = 850$  nm,  $P_t = 250$  mW,  $D_t = 1.5$  cm,  $\eta = 0.025$ ,  $T_s = 0.5$  ns and  $M = 2$ . Note that, for these parameters, a capacity (data rate) of 1 Gbps could be achieved for distances of up to  $\sim 1800$  km.**

The cubesat design will conform to the CDS. The DORA payload will occupy less than 1U of space, easily accommodated in addition to the core subsystems in a 3U design. The cubesat bus for DORA draws on heritage from *Phoenix*, a 3U cubesat with a thermal imaging payload (Rogers et al. 2020). *Phoenix* was designed and built by undergraduate students at Arizona State University and was deployed from the International Space Station in February, 2020. The system was operated successfully from ASU and by several amateurs until a computer fault ended normal operations.

### Subsystems

The onboard computer manages three communications subsystems, two pointing systems, power, auxiliary ground during terrestrial testing, and a high bandwidth data link. Our match to these requirements is the BeagleBone Black. This open source design is available commercially for less than \$100 or with flight heritage packaged into the Pumpkin MBM2. It includes a 1 Gbps Ethernet interface needed to download test data from the payload.

The DORA module requires minimal bus pointing accuracy to close a link. In practice on-orbit testing motivates significant margin. The receiver can determine incoming angles up to an angle roughly set by the deployment angle of the side panels. An attitude determination accuracy better than  $10^\circ$  will provide margin to orient toward the ground station for reception.

When the receiver is well illuminated, the derived angle of arrival can be used to steer the transmitter into alignment. The transmitter is limited to  $\pm 36^\circ$  by the steering mirror actuator, providing no additional attitude accuracy requirement.

A pointing system with these requirements is currently the subject of a trade study. Nighttime operation is required, limiting sensors to earth limb, magnetic, and stellar. We also require a nadir-pointing mode to ensure the DORA payload is oriented towards Earth during communication test passes and prefer a sun-tracking mode to ensure efficient charging. *Phoenix* used an MAI 400 for its ADCS, however this module is no longer available. We are currently considering two ADCS options: the Tensor Tech ADCS100 and the Cube ADCS. Both have specifications that meet our minimum requirements.

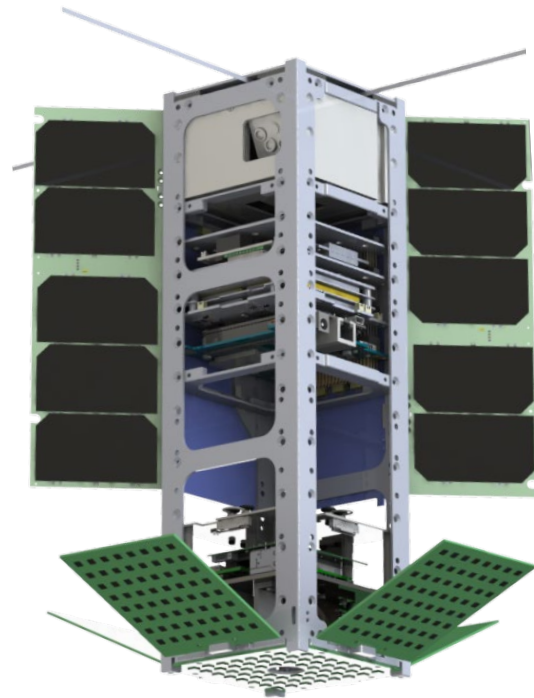


**Figure 8: Rendering of full cubesat. The DORA payload is at the bottom and shown with the aluminum shell hidden.**

The power system of DORA consists of an EPS, batteries, and the solar panels. We elected for components that have already been demonstrated with our on-board computer. Pumpkin has a modified version of the Clydespace 3G EPS that is designed to match the PC104 header of the MBM2. The EPS has 3V, 5V, 12V, and battery voltage busses available. It is also directly compatible with Pumpkin solar panels. We are currently



performing a trade study between the Pumpkin BM2 battery and the Clydespace Optimus battery. The Pumpkin battery has a larger capacity and higher discharge rate, while the Clydespace battery mounts within the PC104 header and comes in multiple sizes. The trade study is pending the completion of a real-time power analysis to determine if we need the extra capacity and discharge rate that the Pumpkin battery provides.

In addition to the ADCS, we will use a Hexagon Novatel OEM719 Multi-Frequency GNSS receiver to provide orbital position and precision timing. This receiver has access to all satellite constellations and has proven flight heritage with cubesat missions. It has an RTK mode that can yield centimeter-level precision. It is small enough to fit on a custom interface board within the PC104 stack, possibly paired up with another component.

The DORA cubesat will use the recently open-sourced OpenLST radio. This radio design was released by Planet (Klofas, 2018). It uses the 70 cm UHF band with a frequency modulation format of 2FSK and has a maximum transmission data rate of 7400 bps at a peak power of 1W. An OpenLST radio can be fabricated for less than \$100 dollars. The drawbacks include limited part availability and the potential instability of an open source project. As part of our evaluation we have made some updates to account for changing conditions since the first design release. The power amplifier in the original design was recently deprecated, we have replaced it with a newer drop-in model. A SAW filter can only be acquired from one company with limited alternatives, hence we have acquired a large stock of spares. We are also updating the ground support software from Python 2 to 3. These and other minor updates are available in our fork of the repository.<sup>1</sup>

The DORA cubesat will use a deployable UHF antenna developed for ASU's LightCube cubesat mission (<http://lightcube.space>). The antenna is expected to fly before DORA, providing some flight heritage and reducing risk. The circular-polarized antenna uses four Nitinol elements deployed by a hot-wire circuit commanded by the OBC.

We also plan on implementing an Eyestar-S3 Simplex as a backup means of communication with the cubesat. The Eyestar communicates with the Globalstar satellite network to provide real-time, always-available access the cubesat. The Globalstar system supports 9 bps data transfer and will primarily be used to broadcast a health heartbeat for the cubesat. The S3 has TRL 8 and, like the

Novatel GNSS receiver, can fit on a custom interface board within the PC104 stack.

The flight software is built on the open-source framework, KubOS, using the Rust programming language. KubOS is a microservice oriented architecture and separates on-board functionality into two levels: services and mission applications. Services are low level applications that provide all hardware interfaces and general background functionality, whereas mission applications implement the high-level control of the satellite. KubOS was chosen for its ease of use and support of the BeagleBone Black as one of the main targets. The central focus of the flight software is error handling and fault containment, which is supported by the KubOS architecture's service-oriented design.

## GROUND STATION

The DORA optical ground terminal (OGT) will be a unique optical transceiver, enabling high speed uplink and downlink with the DORA payload from the ground. The mechanical OGT system consists of three key components. The first is a 200 mm diameter lens, seen in blue in Figure 9. The lens provides a large optical aperture, allowing all the signal power to be focused on the receiver board located internally at the lens focal point, 400 mm back. This feature increases signal strength while minimizing noise and loss. It also decreases the overall cost, as producing an aperture consisting entirely of photodiode receivers would be comparatively expensive.

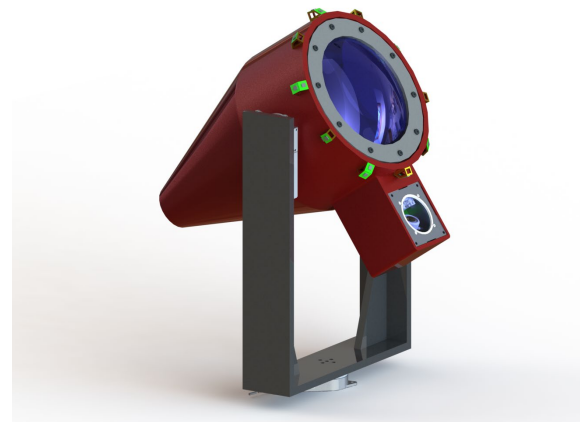


**Figure 9: Optical Ground Terminal**

The second key feature of the OGT is the transmitter seen in the cube below the lens in Figure 9. It is a modified replica of the one on the DORA payload. It uses an optical steering mirror to help point the optical signal directly at the DORA spacecraft in orbit. The only

<sup>1</sup> <https://github.com/InterplanetaryLab/openlst>

modifications are to remove the burn wire mechanisms and the receiver tiles that are on the orbital payload. The receiver tiles are replaced by the final key component of the OGT, a set of 20 receiver boards on independent planes, seen in green around the OGT aperture in Figure 9. The 20 receiver boards are configured in planes representative of a large icosahedron, enabling the AoA algorithm to detect the angle of the incoming optical signal and reorient the OGT in the direction of the oncoming beam.

An optical ground terminal PCB serves as an interface between an FPGA and the optical ground station components. The incoming analog optical signals from the photodiodes on the terminal vertices are digitized and routed to the FPGA. A 16-pin Harwin connector is used to power and interface with the Optotune mirror carrier board.

Ground station software is implemented as an application-oriented design in Rust. The software uses a basic terminal for commanding and receiving, with additional applications to store and display data. Telemetry data is stored in a local PostgreSQL database and displayed using the open-source system, Grafana. Logs received from the spacecraft are stored separately from the telemetry in an influx database and similarly visualized using Chronograf. Each application is made to be independent to increase the degree of fault containment. For example, if an error occurs with the PostgreSQL database, then commanding/receiving and log storage and visualization are all unaffected and the Grafana dashboard would cease to update since there is no new telemetry being stored. The current design allows for new functionality to be easily added or removed as we continue development on the ground software.

## CONCLUSION

In this paper we have presented the design of a widefield optical receiver payload module and associated ground terminal. Widefield optical receivers offer new operational modes for high-speed communication between spacecraft and from orbit to surface, potentially enabling new network architectures in cis-lunar space. They decouple the communication system from spacecraft bus attitude control, making them uniquely suitable for small satellites. Background light needs to be mitigated more carefully in a widefield receiver than for narrow field optical systems. The DORA payload module will be validated in space using a 3U cubesat to demonstrate high-speed links between LEO and a ground terminal on Earth. We anticipate launch in 2023.

## ACKNOWLEDGEMENTS

DORA is supported by NASA SmallSat Technology Partnerships through award 80NSSC20M0086.

## REFERENCES

1. Burleigh, Scott, et al., "Delay-tolerant networking: an approach to interplanetary internet", IEEE Communications Magazine 41.6, 128-136, 2003
2. Cahoy, Kerri et al., "The CubeSat Laser Infrared Crosslink Mission (CLICK)", Proc. SPIE 11180, International Conference on Space Optics — ICSO 2018, 111800Y, July 12, 2019
3. Velazco, Jose, E., "High data rate inter-satellite Omnidirectional Optical Communicator", Proceedings of the Small Satellite Conference, Advanced Concepts I, SSC18-WKI-02, 2018
4. Velazco, Jose E., "Omnidirectional Optical Communicator", IEEE Aerospace Conference 2019, Big Sky, Montana, March 2-9, 2019
5. Rogers et al., "Phoenix: A CubeSat Mission to Study the Impact of Urban Heat Islands Within the U.S.", Proceedings of the Small Satellite Conference, A Look Back: Lessons Learned, SSC20-WKII-04, 2020
6. Starke Jr, E. A. and T. S. J., "Application of modern aluminum alloys to aircraft," Progress in aerospace sciences, vol. 32, no. 2-3, pp. 131-172, 1996
7. The CubeSat Program, "CubeSat Design Specification Revision. 13", California Polytechnic State University, <http://cubesat.org>, 2015
8. Klofas, B., "Planet Releases OpenLST, an Open Radio Solution", <https://www.planet.com/pulse/planet-openlst-radio-solution-for-cubesats/>, <https://github.com/OpenLST>, 2018
9. Hodges, R., "ISARA-integrated solar array and reflectarray CubeSat deployable Ka-band antenna," IEEE International Symposium on Antennas and Propagation & USNC/URSI National Radio Science Meeting, pp. 2141-2142, 2015